

Article

# Influence of Bismaleimide HVA-2 Grafting on the Direct Current Dielectric Properties of XLPE

Chengcheng Zhang \*, Sen Wang, Hong Zhao \* and Xuan Wang

Key Laboratory of Engineering Dielectrics and Its Application, Ministry of Education, Harbin University of Science and Technology, Harbin 150080, China

\* Correspondence: cczh0111@126.com (C.Z.); hongzhao@hrbust.edu.cn (H.Z.)

**Abstract:** In this paper, N, N'-m-phenylene dimaleimide (HVA-2) grafted crosslinked polyethylene (XLPE) insulation materials with different HVA-2 contents were prepared. The grafting, crosslinking, and crystalline structure were characterized by Fourier-transform infrared spectroscopy (FTIR), Soxhlet extraction, and differential scanning calorimetry (DSC), respectively. The space charge distribution, direct current (DC) breakdown strength, and DC conduction current density were tested and the electronic structure was calculated from first-principles. HVA-2 grafting modification can significantly reduce the accumulation of space charges and the conduction current density of XLPE, but have a negative effect on DC breakdown strength. The polar groups of the grafted HVA-2 anchored on XLPE by the grafting reaction can introduce deep traps densely and evenly in XLPE, which would capture and scatter charge carriers, thus reducing the carrier concentration and mobility and further improving the space charge distribution and reducing conduction current density. However, the grafting of HVA-2 can increase the crosslinking extent of XLPE to make the crystallinity decrease and the crystallization inhomogeneous, leading to a certain decrease in the breakdown strength of the grafted XLPE.

**Keywords:** crosslinked polyethylene; grafting; space charge; breakdown; deep traps



**Citation:** Zhang, C.; Wang, S.; Zhao, H.; Wang, X. Influence of Bismaleimide HVA-2 Grafting on the Direct Current Dielectric Properties of XLPE. *Energies* **2023**, *16*, 302. <https://doi.org/10.3390/en16010302>

Academic Editor: Ayman El-Hag

Received: 10 November 2022

Revised: 9 December 2022

Accepted: 17 December 2022

Published: 27 December 2022



**Copyright:** © 2022 by the authors. Licensee MDPI, Basel, Switzerland. This article is an open access article distributed under the terms and conditions of the Creative Commons Attribution (CC BY) license (<https://creativecommons.org/licenses/by/4.0/>).

## 1. Introduction

With the emergence of the concept of ultra high voltage (UHV), there were many discussions about UHV direct current (DC) and alternating current (AC) transmission. The AC voltage levels can be converted by means of step-up or step-down voltage from transformers, which brings great convenience to the distribution of electric energy. However, there are losses caused by the impedance of the conductive core and AC inductance in the AC transmission process [1]. There is only loss of the conductive core in the DC transmission process, and the loss can be diminished by increasing the voltage level. Therefore, the DC transmission can be used in long-distance, high-capacity, and low-loss power transmission systems [2,3]. In recent years, some DC transmission projects were constructed one after another. Under the background of a “dual carbon” goal, the DC transmission projects will reach an unprecedented scale and contribute to the new energy industry.

Crosslinked polyethylene (XLPE) is a thermosetting polymer developed based on polyethylene (PE), which is an indispensable material for medium and high-voltage DC (HVDC) cables at present. It not only has the advantages of good electrical insulation and lightweight, the same as PE, but it also has excellent heat resistance, physical and mechanical properties, etc. [4]. However, under a DC electric field, space charges can be formed in a XLPE insulation layer through the injection by the electrode and the dissociation of impurities or crosslinking by-products introduced during the preparation of XLPE, which could cause local electric distortion and threaten the stability of HVDC cable operation [5]. Therefore, it plays an important role in the safe and stable operation of DC transmission systems to restrain the space charge accumulation and improve DC dielectric properties of XLPE.

Grafting polar groups onto XLPE can suppress space charge accumulation in XLPE. Suh K.S. [6] and Lee S.H. [7] et al. tested the dielectric properties of acrylic acid (AA) and maleic anhydride (MAH) grafted low-density polyethylene (LDPE) and found that the amount of space charge accumulation in the grafted LDPE was significantly decreased. Zhao X.D. [8] et al. prepared allyl chloroacetate (CAAE) grafted XLPE and found that the grafting can reduce the accumulation of space charges, decrease the conductivity, and improve DC breakdown strength, and 1.0 wt.% CAAE grafted XLPE had the most excellent dielectric properties. When antioxidant MC was grafted onto LDPE, the prepared specimens had better DC dielectric properties than LDPE, such as the reduced space charge amount and conduction current density, and improved DC breakdown strength [9]. The polar groups, such as carbonyl and ester groups were introduced into the macromolecular chain of XLPE insulation materials through the grafting reaction, which can form a large number of deep traps in the specimen to restrict the movement of carriers, thereby enhancing DC dielectric properties [10,11].

The existing studies revealed that the maleimide has an excellent inhibiting capability for space charge accumulation in PE due to its structure and the polar groups it contains. N, N'-m-phenylene dimaleimide (HVA-2), as its derivative, has more polar groups, such as carbonyl and amines groups. Therefore, it is reasonable to believe that it may play a greater role in inhibiting the accumulation of space charges [12,13]. HVA-2 could be grafted onto XLPE macromolecular chains through carbon-carbon double bonds during the crosslinking process. At the same time, HVA-2 may promote the crosslinking reaction as a crosslinking co-agent. Therefore, in this paper, HVA-2 grafted XLPE was prepared and the effect of HVA-2 grafting on DC dielectric properties of XLPE insulation materials was researched.

## 2. Experimental

### 2.1. Materials

Low-density polyethylene (LDPE, LD200GH) used as a base material was purchased from Sinopec Beijing Yanshan Company, Beijing, China, and the melt flow index and the density are 2.0 g/10 min and 0.922 g/cm<sup>3</sup>, respectively. The crosslinker dicumyl peroxide (DCP) was supplied by Akzo Nobel N.V., Amsterdam, Netherlands. N, N'-m-phenylene dimaleimide (HVA-2) was provided by J&K Scientific Ltd., Beijing, China and the molecular structure is represented in Figure 1.

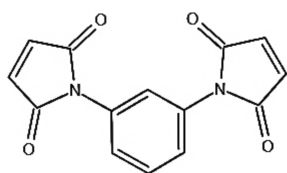


**Figure 1.** Molecular structure of N, N'-m-phenylene dimaleimide.

### 2.2. Preparation of HVA Grafted XLPE Specimen

A certain quantity of LDPE pellets were weighed and put into the torque rheometer at 110 °C and a motor speed of 50 r/min. After LDPE was completely melted, a certain amount of HVA-2 was added in and blended for around 5 min. Finally, 1.8 phr (phr: parts per hundreds of resin) DCP was added in and blended for another 3 min to obtain a blend of HVA-2 and LDPE. The mixture was hot compression moulded on a flat vulcanizing machine under 15 MPa at 110 °C, and then transferred to 175 °C at the same pressure for 30 min to complete the crosslinking and grafting reaction; 0, 0.3, 0.5, 1.0 and 1.5 phr HVA-2 grafted XLPE were obtained and denoted as XLPE, XLPE-g-0.3HVA, XLPE-g-0.5HVA, XLPE-g-1.0HVA, and XLPE-g-1.5HVA. Before the measurement of electrical properties, the specimen was placed in a vacuum oven at 80 °C for 24 h to eliminate the influence of crosslinking by-products arising from the crosslinking reaction process and unsuccessfully grafted HVA-2 on the measurement results as much as possible.

### 2.3. Characterization

To validate the grafting reaction of HVA-2 onto the macromolecular chain of XLPE, Fourier-transform infrared spectroscopy (FTIR) of polymer specimens before and after the grafting and crosslinking reaction and HVA-2 was measured by the transmission mode of a spectrometer (FT/IR-6100, Jasco, Tokyo, Japan) in the wavenumber range from 2000 to 400  $\text{cm}^{-1}$  with the resolution of 2  $\text{cm}^{-1}$ . The thickness of polymer specimens was about 300  $\mu\text{m}$ . For HVA-2 powder, a potassium bromide (KBr) tablet containing HVA-2 was used for the measurement.

The Soxhlet extraction method was used to measure the gel content [14]. A certain number of specimens were placed into a stainless steel mesh bag with the mass of  $M_1$ . The stainless steel mesh bag and specimens with the total mass of  $M_2$  were refluxed in boiling xylene solution for about 10 h. After extraction, they were dried at 150  $^{\circ}\text{C}$  in a vacuum oven for about 2 h to make the remaining xylene solution completely volatilized, and then were weighed and recorded as  $M_3$ . The gel content of the specimen was calculated by Equation (1) and the average value was calculated after three repeated measurements for each kind of material.

$$\text{Gel Content (\%)} = \frac{M_3 - M_1}{M_2 - M_1} \times 100\% \quad (1)$$

The melting–crystallization curves were tested by a differential scanning calorimeter (DSC 1, Mettler Toledo, Zurich, Switzerland). The specimen was heated to 140  $^{\circ}\text{C}$  from room temperature at 10  $^{\circ}\text{C}/\text{min}$  under high purity nitrogen protection, and kept for 2 min to eliminate the thermal history. Next, under the same rate, the specimen was cooled to 25  $^{\circ}\text{C}$ , and finally was heated to 140  $^{\circ}\text{C}$  again to obtain the crystallization and melting curves. Based on the melting curve, the crystallinity was calculated according to Equation (2).

$$X_c = \frac{\Delta H_m}{\Delta H_{100}} \times 100\% \quad (2)$$

where  $\Delta H_m$  is the melting enthalpy of the specimen normalized by weight, and  $\Delta H_{100}$  is the melting enthalpy of 100% crystalline polyethylene, which is taken as 293.6 J/g [15].

### 2.4. Direct Current Dielectric Properties Measurement

The space charge distribution in the specimen was tested by a pulsed electro-acoustic (PEA) system (PEA-01, Shanghai Xiangtie Electromechanical Equipment Co., Ltd., Shanghai, China). The specimen was supplied with a 3 kV/mm DC electric field for calibration. The thickness of specimens was about 300  $\mu\text{m}$ . In the measurement process, the specimen was supplied with a 40 kV/mm DC electric field for 40 min, and then short-circuited for 30 min. The distribution of space charges in the specimen during the polarization and depolarization were obtained and recorded through the data processing.

DC breakdown strength was measured using two opposing asymmetrical cylindrical electrodes with the diameter of 25 mm for the upper electrode and 75 mm for the lower electrode at the temperature of 25, 50, and 70  $^{\circ}\text{C}$ . The thickness of specimens was about 100  $\mu\text{m}$ . The specimen clamped with the two cylindrical electrodes was immersed in the silicone oil with a constant temperature. Then, the specimen was supplied with a continuously increasing DC electric field at 600 V/s until broken down. The experimental data of the breakdown strengths were processed according to the two-parameter Weibull distribution, as shown in Equation (3) [16].

$$P = 1 - \exp \left[ - \left( \frac{E}{E_0} \right)^\beta \right]. \quad (3)$$

where  $P$  is the cumulative failure probability;  $E$  is the actual breakdown strength when the electric field varies uniformly with time;  $E_0$  is the scale parameter of Weibull distribution,

indicating the characteristic breakdown strength at the 63.2% cumulative failure probability; and  $\beta$  is the shape parameter relating to the data scatter.

The measurement of the DC electrical conduction current was carried out at 25, 50, and 70 °C on a three-electrode system. The thickness of specimens was about 200  $\mu\text{m}$ . Aluminum was vacuum-evaporated on both sides of the specimen before the measurement. The specimen was subjected to a DC electric field ranging from 1 to 50 kV/mm, and the measuring time at each electric field lasted for about 15 min to reach a steady state. The quasi-stationary current was collected by a picoammeter (EST122, EST Technology Co., Limited., Beijing, China).

### 2.5. First-Principles Calculations

The band-edge features and trap states were investigated by the electronic density of states calculated by first-principles. The calculations were carried out using the all-electron and numerical atomorbitals schemes in the DMol 3 program of the Materials Studio 8.0 software package. On the basis of rotational isomeric state (RIS) model, the molecular models of PE with the polymerization degree of 20 were initially established with random distributed torsion. The HVA-2 molecule was grafted onto the central position of the PE backbone chain. The established initial polymer conformations were geometrically optimized through the total energy functional minimization calculated by first-principles to realize relaxation.

## 3. Results and Discussion

FTIR spectra of HVA-2, crosslinkable PE, and crosslinkable PE containing 1.5 phr HVA before and after grafting and crosslinking are represented in Figure 2. For the FTIR spectrum of HVA-2, the absorption peaks at 1607, 1594, 1500, and 1455  $\text{cm}^{-1}$  were attributed to the skeletal vibration of the aromatic ring, the peaks at 1722, 1149, and 827  $\text{cm}^{-1}$  were assigned to the carbonyl stretching vibration, the C-N stretching vibration of the imide group, and the =C-H wagging vibration of the vinylene group [9,17]. After HVA-2 was grafted onto XLPE, the absorption peaks of the aromatic ring at 1607 and 1500  $\text{cm}^{-1}$  and carbonyl groups at 1722  $\text{cm}^{-1}$  emerged in XLPE, and the peak at 1149  $\text{cm}^{-1}$  was broadened and shifted to 1181  $\text{cm}^{-1}$ , from which it can be judged that HVA-2 molecules were introduced in XLPE. Comparing the FTIR spectra of crosslinkable PE containing HVA-2 before and after grafting and crosslinking, it was found that the =C-H absorption peak of the vinylene group of HVA-2 at 827  $\text{cm}^{-1}$  in crosslinkable PE containing HVA-2 disappeared in HVA-2 grafted XLPE after the grafting and crosslinking reaction. FTIR spectra analysis indicated that the C=C bond in the HVA-2 molecule was broken in the reaction, and furthermore that the HVA-2 molecule was successfully grafted onto the XLPE macromolecular chain through free radical addition reaction.

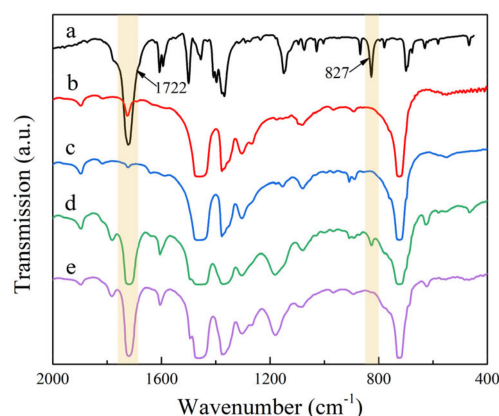


**Figure 2.** FTIR spectra of (a) HVA-2, (b) crosslinkable PE, (c) XLPE, (d) crosslinkable PE containing HVA-2, and (e) XLPE-g-HVA.

The gel contents of XLPE and HVA-2 grafted XLPE with different HVA-2 contents are shown in Table 1. The gel content of XLPE-g-HVA was larger than that of XLPE, of which the gel content of the grafted XLPE with 1.5 phr HVA-2 was the largest. The HVA-2 molecule contains two unsaturated double bonds, which can link two PE macromolecular chains and play a role in promoting the crosslinking reaction in the peroxide crosslinking system [12], making the crosslinking extent of the HVA-2 grafted XLPE specimens slightly higher than that of XLPE. Thus, HVA-2 are used as a crosslinking co-agent in many situations. In this paper, HVA-2 played a dual role as a crosslinking co-agent and grafting monomer, which not only increased the crosslinking extent, but also was grafted onto the XLPE macromolecular chain as a branch chain.

**Table 1.** Gel contents of XLPE and HVA-2 grafted XLPE.

Materials	Gel Content
XLPE	89%
XLPE-g-0.3HVA	92.4%
XLPE-g-0.5HVA	91.5%
XLPE-g-1.0HVA	91.2%
XLPE-g-1.5HVA	93.8%

The crystallization and melting curves of XLPE and HVA-2 grafted XLPE with different HVA-2 contents are shown in Figure 3. The melt and crystallization parameters are summarized in Table 2. The crystallization temperature of HVA-2 grafted XLPE was somewhat lower than that of XLPE, and there was no obvious variation in melting temperature. The crystallinity of HVA-2 grafted XLPE was lower than that of XLPE. As the crosslinking extent of XLPE increased, the crosslinking network nodes increased, which can prevent the movement and regular arrangement of PE macromolecular chains, thus inhibiting the crystallization process. Therefore, the crystallization temperature and the crystallinity decreased [18,19].

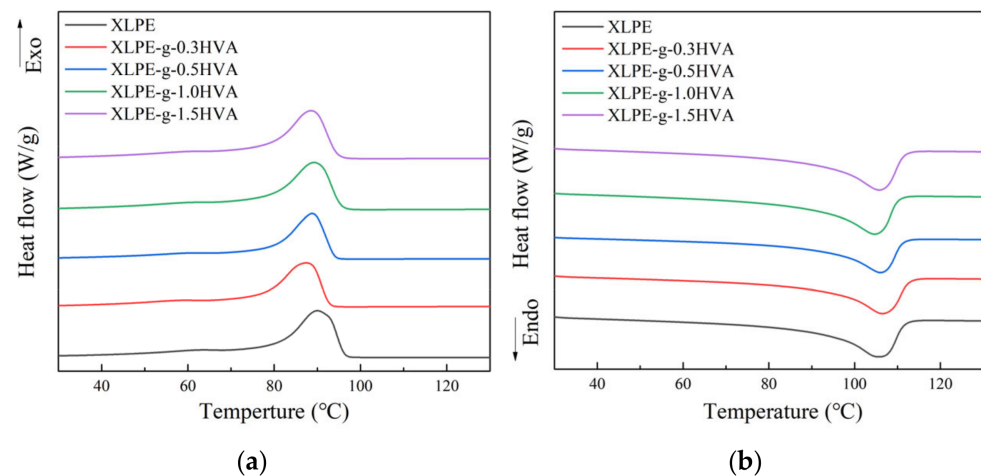


**Figure 3.** DSC curves of XLPE and HVA-2 grafted XLPE. (a) Crystallization and (b) melting.

**Table 2.** Melting and crystallization parameters of XLPE and HVA-2 grafted XLPE.

Materials	Crystallization Temperature (°C)	Melting Temperature (°C)	Crystallinity (%)
XLPE	90.2	105.7	36.7
XLPE-g-0.3HVA	87.5	106.0	34.0
XLPE-g-0.5HVA	89.0	106.3	35.3
XLPE-g-1.0HVA	89.4	105.8	35.7
XLPE-g-1.5HVA	88.0	105.2	33.3

Figure 4 shows the space charge distributions of XLPE and HVA-2 grafted XLPE during polarization at 40 kV/mm and the depolarization process. In Figure 4a,b, a certain quantity of homocharges were injected from the cathode, the heterocharges accumulated around the anode, and a large number of positive space charge packets appeared inside the XLPE specimen after polarization. The dissociation of impurities or crosslinking by-products under an electric field may be the primary source of heterocharges at room temperature. Additionally, the charges injected from the electrodes may cross the specimen to the counter electrodes and be blocked or partially blocked at the electrode interface due to the interface potential barrier, forming the heterocharges around the counter electrodes [20]. During short circuit process, the space charges near the electrodes and inside the specimen decayed gradually with the short circuit time increasing. After short circuiting for 1800 s, the density of homocharges around the cathode, heterocharges around the anode, and positive space charge packets inside the specimen dropped by 66.6%, 80.0%, and 71.1%, respectively.

In the XLPE-g-0.3HVA specimen, a small quantity of homocharges were injected from both the cathode and anode, and there were some positive space charge packets inside the specimen, but the amount of space charges in total decreased significantly compared with that of XLPE, as shown in Figure 4c,d. During short circuit, the space charges hardly dissipated as the short circuit time increased. When HVA-2 content was 0.5 phr, the distribution and amount of space charges in the specimen were almost similar to that of XLPE-g-0.3HVA. As the HVA-2 content increased to 1.0 phr, the amount of homocharges near the cathode in the specimen decreased dramatically, while the homocharges near the anode increased, and the positive space charges inside the specimen decreased (shown in Figure 4h). The amount of homocharges around the anode in the specimen continued to increase as HVA-2 content increased to 1.5 phr, and meanwhile, the positive space charges inside the specimen further declined. Similarly, the space charges decayed slowly in HVA-2 grafted XLPE with 0.5, 1.0, and 1.5 phr HVA-2 during short circuit. It was speculated that HVA-2 grafting modification could introduce deep traps in XLPE, and the charges in the deep traps were difficult to be detrapped during short circuit, resulting in slow charge attenuation [21–23].

To validate the existence of deep traps in HVA-2 grafted XLPE further, the band edge features and trap states of PE and HVA-2 grafted PE were investigated by the calculation of electronic structures, and the results are shown in Figure 5. After HVA-2 was grafted onto PE, three new electronic bound states emerged in the energy bandgap of PE. Two unoccupied bound states were below the conduction band edge as electron traps with the depth of 2.12 and 0.71 eV, and one bound state above the valence band edge merged to the energy band, resulting in the top of the valence band rising. The depth of traps at 2.12 eV was deeper than that introduced by grafting antioxidant MC, maleic anhydride, chloroacetic acid allyl ester, trimethylolpropane trimethacrylate, etc., obtained from first-principles calculations, and the deep traps can bind the charges to suppress space charge accumulation and reduce the mobility of charge carriers through the scattering effect [8,9,22,24].

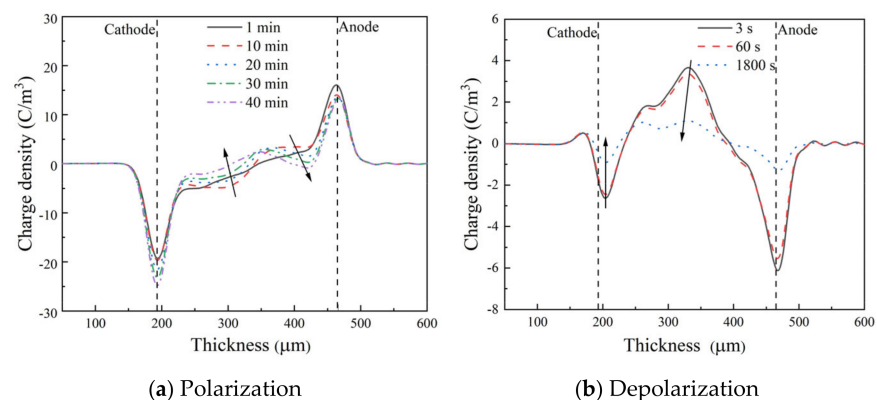
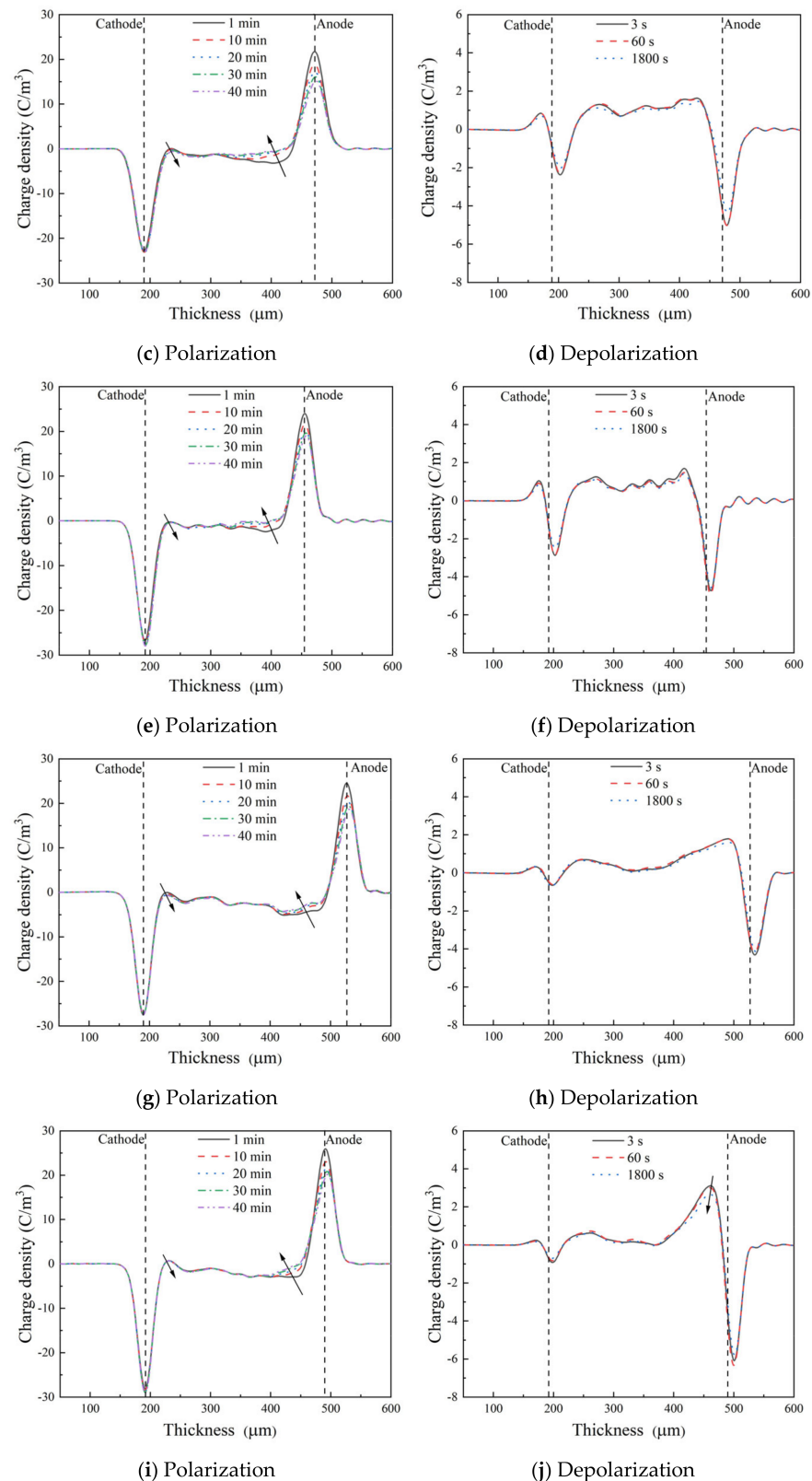


Figure 4. Cont.



**Figure 4.** Space charge distributions of XLPE and HVA-2 grafted XLPE; (a,b) corresponding to XLPE, (c,d) to XLPE-g-0.3HVA, (e,f) to XLPE-g-0.5HVA, (g,h) to XLPE-g-1.0HVA, and (i,j) to XLPE-g-1.5HVA.

In comparison to XLPE, HVA-2 grafted XLPE with different HVA-2 contents can all suppress space charge accumulation in XLPE to a different extent, and the space charge density of the grafted XLPE was dramatically reduced during the polarization process

under 40 kV/mm. The polar groups, such as carbonyl and tertiary amine groups existing in the HVA-2 molecular structure can be anchored onto XLPE macromolecular chains by the grafting reaction and introduce deep traps in XLPE densely and evenly. Under the DC electric field, the deep traps can capture the homocharges injected by the electrode and form an immobile homocharge layer to reduce the effective electric field between the electrode and the charge layer and increase the potential barrier for the injection of charges, thus inhibiting further injection of charges. At the same time, the deep traps can capture the charges and restrict the movement of trapped charges to achieve the purpose of reducing the internal free charges [6–9,23,25]. As a result, the amount of the homocharges and heterocharges reduced and the space charge distribution was improved inside the specimen.

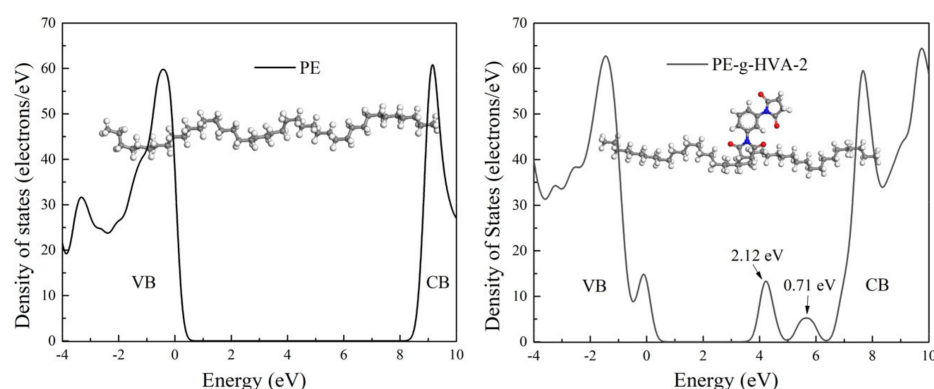


**Figure 5.** The density of states for PE and HVA-2 grafted PE (CB = conduction band, VB = valence band).

The Weibull distributions of DC breakdown strengths of XLPE and HVA-2 grafted XLPE at 25, 50, and 70 °C are represented in Figure 6. DC breakdown strengths of XLPE after HVA-2 grafting modification at 25 and 50 °C reduced significantly, and the breakdown strength of the grafted XLPE fell more obviously as the HVA-2 content increased. The breakdown strength of XLPE-g-1.5HVA dropped by 46.4% and 37.1%, respectively, compared with that of XLPE at 25 and 50 °C. However, at 70 °C, DC breakdown strength of HVA-2 grafted XLPE changed little, and increased firstly and then decreased with the HVA-2 content increasing. When the content of HVA-2 was 0.5 phr, the breakdown strength was the largest, 222.1 kV/mm.

Overall, HVA-2 grafting would make the breakdown strength of XLPE decrease to some extent at the low temperature region, and the decrease was positively correlated with the content of HVA-2. The unsuccessfully grafted HVA-2 cannot be completely removed and become the impurity inside the specimen, releasing some impurity ions under the electric field, which would negatively affect the breakdown strength [18]. Although the deep traps introduced in HVA-2 grafted XLPE can capture and scatter the charge carriers to positively affect the breakdown strength, the physical state of polymers can also affect the breakdown strength significantly. HVA-2 grafting can increase the crosslinking extent of XLPE, and the network nodes disturbed the chain motion of PE macromolecules, resulting in the formation of irregular-sized spherulites and incomplete structure in the crystallization region, as well as loose structure in the amorphous region [26]. Additionally, the crystallinity of HVA-2 grafted XLPE was obviously reduced, and the grafted XLPE had a larger proportion of amorphous regions. As a result, the free volume increased and the charge transport was enhanced in HVA-2 grafted XLPE, which made the charge carriers obtain energy more easily and the breakdown strength reduce [27]. The superposition effect of high electric field impurity dissociation combined with crystalline inhomogeneity and a larger amorphous region exceeded the trap effect of polar groups, resulting in the breakdown strength of HVA-2 grafted XLPE decreasing compared with that of XLPE.

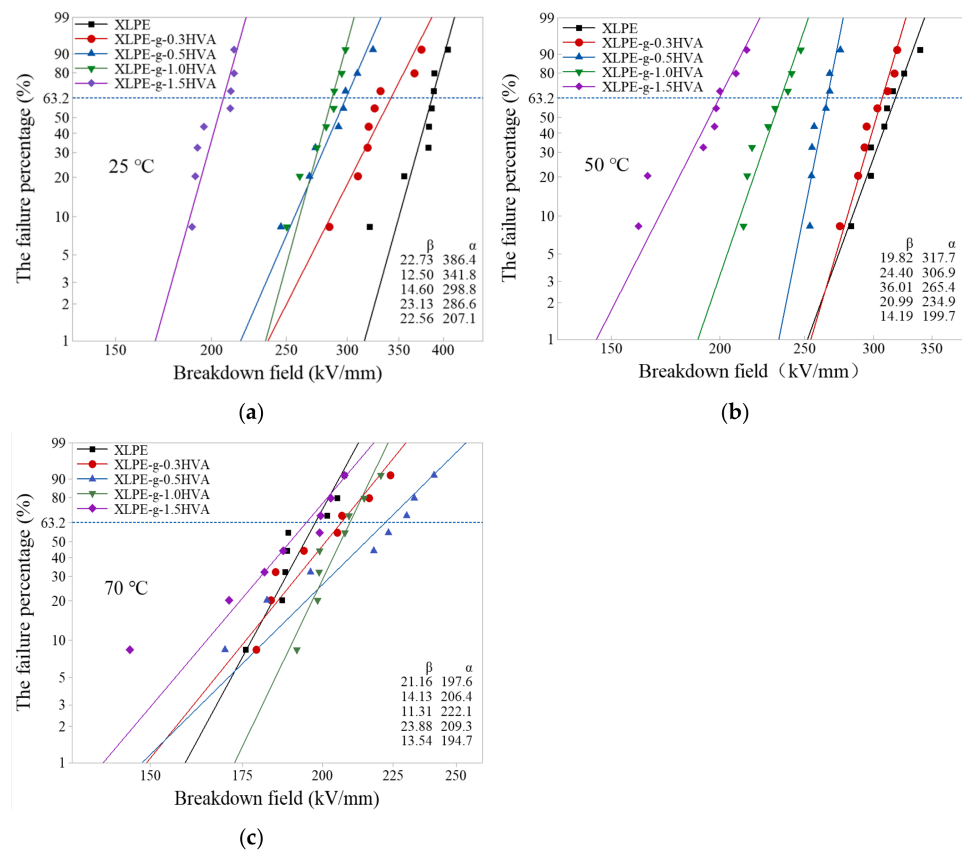


**Figure 6.** Weibull distributions of DC breakdown strengths of XLPE and HVA-2 grafted XLPE. (a) 25 °C, (b) 50 °C, and (c) 70 °C.

The breakdown strength of XLPE and HVA-2 grafted XLPE decreased to different extents with the increase in the test temperature, and the results are represented in Figure 7. XLPE had the largest decline in DC breakdown strength. With the content of HVA-2 increased, the decline in the breakdown strength of the grafted XLPE slowed down, and the breakdown strength of the grafted XLPE with 1.5 phr HVA-2 showed just a slight change; it indicated that the temperature dependence of the breakdown strength of HVA-2 grafted XLPE was smaller than that of XLPE. At 70 °C, the breakdown strength of HVA-2 grafted XLPE was higher at lower HVA-2 contents than that of XLPE. During the operation of the cables, the insulation layer temperature will vary with the load conditions and can reach 70 °C, and may be even higher in case of short circuit and emergency. The breakdown behavior of insulation materials at a higher temperature is especially important and the breakdown strength of HVA-2 grafted XLPE can be enhanced at a higher temperature. Therefore, it is more important to achieve a positive better space charge distribution by introducing deep traps than a negative reduction in the breakdown strength at a lower temperature.

The logarithmic relationship curves of conduction current density and electric field (J-E) of XLPE and HVA-2 grafted XLPE at 30, 50, and 70 °C are shown in Figure 8. At different test temperatures, the conduction current density of HVA-2 grafted XLPE with different HVA-2 contents decreased significantly compared with that of XLPE in the whole electric field. At 30 °C, the conduction current density of HVA-2 grafted XLPE exhibited a trend of decreasing firstly and then increasing with the increase in HVA-2 content, and reached the minimum value with 1.0 phr HVA-2. Excess unsuccessfully grafted HVA-2 dissociated to form impurity ions under the electric field, which increased the amount of carriers in the specimen, thus leading to a slight increase in the conduction current density of XLPE-g-1.5HVA. At 50 and 70 °C, the trend of the conduction current density

was approximately the same with that at 30 °C, except that the conduction current density values of XLPE-g-1.5HVA were very close to those of XLPE-g-1.0HVA.

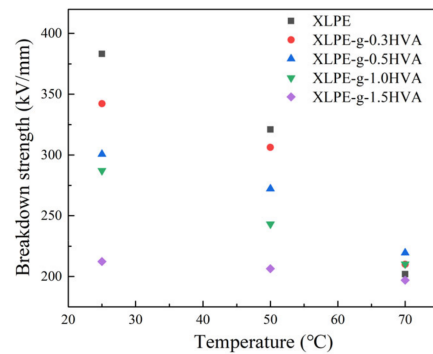


**Figure 7.** DC breakdown strength curves of XLPE and HVA-2 grafted XLPE as a function of temperature.

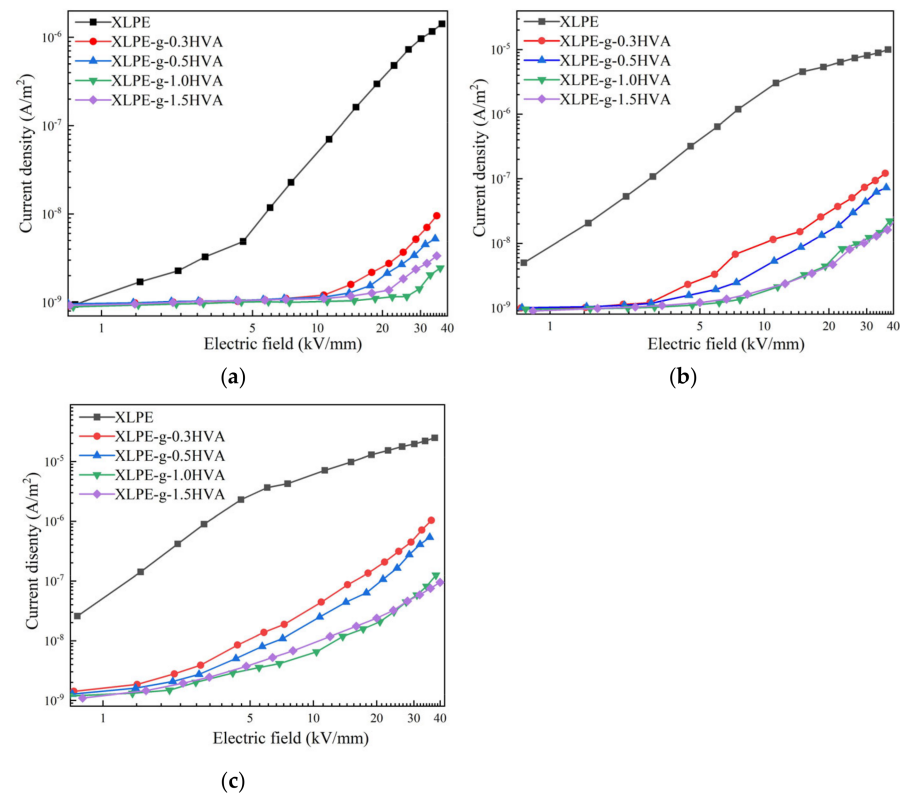


**Figure 8.** Conduction current density curves of XLPE and HVA-2 grafted XLPE; (a) 25 °C, (b) 50 °C, and (c) 70 °C.

Moreover, it was found that the threshold field between low field and high field regions of HVA-2 grafted XLPE increased significantly at 30 °C, and increased firstly and then decreased with the HVA-2 content increasing. The threshold field is positively correlated with the trap depth in the insulation materials [28]. Therefore, it can be concluded that HVA-2 grafting modification can introduce deep traps with a higher energy level in XLPE, which coincided with the results obtained by the space charge measurement and the calculation for density of state. These deep traps can capture and scatter the charge carriers in the charge transport process to restrict the movement of carriers, and also enhance the potential barrier for charge injection to suppress their further injection, which would lead to the amount and mobility of charge carriers decreasing. Therefore, the conduction current density of HVA-2 grafted XLPE reduced [29].

The conduction current density of XLPE and HVA-2 grafted XLPE increased with the increase in the temperature and the threshold field decreased. The threshold field was not even detected at a higher temperature, which may indicate that the rate of charge injection increased with the temperature. In addition, under the high temperature condition, more impurities dissociated under a high temperature condition, and some trapped low-energy carriers gained enough energy to be detrapped from the traps [28]. As a result, the amount and mobility of charge carriers increased, resulting in the conduction current density increasing at a higher temperature.

#### 4. Conclusions

In this paper, HVA-2 grafted XLPE insulation materials with different HVA-2 contents were prepared with LDPE as base material. HVA-2 grafting modification can slightly increase the crosslinking extent of XLPE and reduce the crystallinity. The polar groups of the grafted HVA-2 anchored on XLPE macromolecules would introduce deep traps densely and evenly in XLPE. The deep traps can capture the charges injected from the electrode to reduce the amount of injected charge carriers, and restrict the movement of trapped charges to suppress space charge accumulation and reduce the conduction current density at different test temperatures. DC breakdown strength of the grafted XLPE decreased due to the superposition effect of the crystalline inhomogeneity, larger amorphous region, and impurity dissociation, but the temperature dependence of the breakdown strength was significantly reduced compared with that of XLPE. At the higher temperature above 50 °C, the breakdown strengths of HVA-2 grafted XLPE with lower HVA-2 contents were even higher than that of XLPE. Therefore, grafting HVA-2 onto XLPE was beneficial on DC dielectric properties of XLPE, and 0.5 phr addition content was relatively most appropriate based on comprehensive consideration of space charge distribution, breakdown strength, conduction current density, and economic benefit. HVA-2 grafted XLPE may be expected to be applied to HVDC cable XLPE insulation materials.

**Author Contributions:** Conceptualization, C.Z. and H.Z.; funding acquisition, X.W.; investigation and methodology, S.W. and C.Z.; supervision, C.Z.; writing—original draft, S.W.; writing—review and editing, C.Z. All authors have read and agreed to the published version of the manuscript.

**Funding:** This research was funded by National Natural Science Foundation of China, No. U20A20307 and 51707049.

**Data Availability Statement:** Not applicable.

**Conflicts of Interest:** The authors declare no conflict of interest.

#### References

1. Borioli, E.; Brenna, M.; Faranda, R.; Simioli, G. Comparison between the electrical capabilities of the cables used in LV AC and DC power lines. In Proceedings of the 2004 11th international conference on harmonics and quality of power, Lake Placid, NY, USA, 12–15 September 2004.
2. Agelidis, V.G.; Demetriades, G.D.; Flourentzou, N. Recent advances in high-voltage direct-current power transmission systems. In Proceedings of the 2006 IEEE International Conference on Industrial Technology, Mumbai, India, 15–17 December 2006.
3. Jovicic, D.; Van Hertem, D.; Linden, K.; Taisne, G.; Grieshaber, W. Feasibility of DC transmission networks. In Proceedings of the 2011 2nd IEEE PES International Conference and Exhibition on Innovative Smart Grid Technologies, Manchester, UK, 5–7 December 2011.
4. Zhou, Y.; Peng, S.; Hu, J.; He, J.L. Polymeric insulation materials for HVDC cables: Development, challenges and future perspective. *IEEE Trans. Dielectr. Electr. Insul.* **2017**, *24*, 1308–1318. [[CrossRef](#)]
5. Mizutani, T. Space charge measurement techniques and space charge in polyethylene. *IEEE Trans. Dielectr. Electr. Insul.* **1994**, *1*, 923–933. [[CrossRef](#)]
6. Suh, K.S.; Yoon, H.G.; Lee, C.R.; Okamoto, T. Space charge behavior of acrylic monomer-grafted polyethylene. *IEEE Trans. Dielectr. Electr. Insul.* **1999**, *6*, 282–287. [[CrossRef](#)]
7. Lee, S.H.; Park, J.K.; Han, J.H.; Suh, K.S. Space charge behaviour in maleic anhydride grafted polyethylene/ethylene-vinyl-acetate copolymer laminates. *J. Phys. D* **1997**, *30*, 1–4. [[CrossRef](#)]
8. Zhao, X.D.; Sun, W.F.; Zhao, H. Enhanced insulation performances of crosslinked polyethylene modified by chemically grafting chloroacetic acid allyl ester. *Polymers* **2019**, *11*, 592. [[CrossRef](#)]

9. Zhang, C.C.; Wang, T.T.; Sun, W.F.; Li, C.Y.; Zhao, H. Grafting of antioxidant onto polyethylene to improve DC dielectric and thermal aging properties. *IEEE Trans. Dielectr. Electr. Insul.* **2021**, *28*, 541–549. [[CrossRef](#)]
10. Liang, Y.; Liu, L.Z.; Zhang, W.L.; Weng, L.; Hu, D.S.; Li, C.Y. Preparation and electrical properties of 4-acetoxystyrene grafted polypropylene for HVDC cable insulation. *J. Mater. Sci. Mater. Electron.* **2020**, *31*, 3890–3898. [[CrossRef](#)]
11. Zha, J.W.; Wu, Y.H.; Wang, S.J.; Wu, D.H.; Yan, H.D.; Dang, Z.M. Improvement of space charge suppression of polypropylene for potential application in HVDC cables. *IEEE Trans. Dielectr. Electr. Insul.* **2016**, *23*, 2337–2343. [[CrossRef](#)]
12. Wang, Y.; Zhang, H.; Zhao, H.; An, T.; Du, X.; Lu, Y.; Chen, Z.G. Theoretical study on the grafting reaction of maleimide and its derivatives to polyethylene in the UV radiation cross-linking process. *Struct. Chem.* **2019**, *30*, 1033–1039. [[CrossRef](#)]
13. Zhao, H.; Chen, J.Q.; Zhang, H.; Shang, Y.; Wang, X.; Han, B.Z.; Li, Z.S. Theoretical study on the reaction of triallyl isocyanurate in the UV radiation cross-linking of polyethylene. *RSC Adv.* **2017**, *7*, 37095–37104. [[CrossRef](#)]
14. Kampaouris, E.M.; Andreopoulos, A.G. Gel content determination in cross-linked polyethylene. *Biomaterials* **1989**, *10*, 206–208. [[CrossRef](#)] [[PubMed](#)]
15. Ma, D.; Hugener, T.A.; Siegel, R.W.; Christerson, A.; Mårtensson, E.; Önnby, C.; Schadler, L.S. Influence of nanoparticle surface modification on the electrical behaviour of polyethylene nanocomposites. *Nanotechnology* **2005**, *16*, 724–731.
16. Cacciari, M.; Mazzanti, G.; Montanari, G.C. Weibull statistics in short-term dielectric breakdown of thin polyethylene films. *IEEE Trans. Dielectr. Electr. Insul.* **1994**, *1*, 153–159. [[CrossRef](#)]
17. Štirn, Ž.; Ručigaj, A.; Krajnc, M. Innovative approach using aminomaleimide for unlocking phenolic diversity in high-performance maleimidobenzoxazine resins. *Polymer* **2017**, *120*, 129–140. [[CrossRef](#)]
18. Yan, Z.M.; Yang, K.; Wang, S.H.; Li, J.Y. Crosslinking dependence of trap distribution and breakdown performance of crosslinked polyethylene. *J. Mater. Sci. Mater. Electron.* **2019**, *30*, 20605–20613. [[CrossRef](#)]
19. Sahyoun, J.; Crepet, A.; Gouanve, F.; Keromnes, L.; Espuche, E. Diffusion mechanism of byproducts resulting from the peroxide crosslinking of polyethylene. *J. Appl. Polym. Sci.* **2017**, *134*, 44525. [[CrossRef](#)]
20. Montanari, G.C.; Fabiani, D.; Dissado, L.A. A new conduction phenomenon observed in polyethylene and epoxy resin: Ultra-fast soliton conduction. *J. Polym. Sci. B Polym. Phys.* **2011**, *49*, 1173–1182. [[CrossRef](#)]
21. Li, J.; Han, C.L.; Du, B.X.; Takada, T. Deep trap sites suppressing space charge injection in polycyclic aromatic compounds doped XLPE composite. *IET Nanodielectrics* **2020**, *3*, 10–13. [[CrossRef](#)]
22. Zhao, X.D.; Zhao, H.; Sun, W.F. Significantly improved electrical properties of crosslinked polyethylene modified by UV-initiated grafting MAH. *Polymers* **2020**, *12*, 62. [[CrossRef](#)]
23. Yuan, C.; Hu, S.X.; Li, Y.S.; Yang, M.C.; Li, J.L.; Cheng, S.; Hu, J.; Li, Q.; He, J.L. Properties of grafting methyl acrylate on charge transport in polypropylene. In Proceedings of the 2020 IEEE International Conference on High Voltage Engineering and Application, Beijing, China, 6–10 September 2020.
24. Peng, Q.; Chen, J.Q.; Sun, W.F.; Zhao, H. Improved DC dielectric performance of photon-initiated crosslinking polyethylene with TMPTMA auxiliary agent. *Materials* **2019**, *12*, 3540.
25. Zhang, C.C.; Chang, J.X.; Zhang, H.Y.; Li, C.Y.; Zhao, H. Improved direct current electrical properties of crosslinked polyethylene modified with the polar group compound. *Polymers* **2019**, *11*, 1624. [[CrossRef](#)] [[PubMed](#)]
26. Gulmine, J.V.; Akcelrud, L. Correlations between the processing variables and morphology of crosslinked polyethylene. *J. Appl. Polym. Sci.* **2004**, *94*, 222–230. [[CrossRef](#)]
27. Ieda, M. Dielectric breakdown process of polymers. *IEEE Trans. Electr. Insul.* **1980**, *15*, 206–224. [[CrossRef](#)]
28. Montanari, G.C. The electrical degradation threshold of polyethylene investigated by space charge and conduction current measurements. *IEEE Trans. Dielectr. Electr. Insul.* **2000**, *7*, 309–315. [[CrossRef](#)]
29. Wang, W.W.; Min, D.M.; Li, S.T. Understanding the conduction and breakdown properties of polyethylene nanodielectrics: Effect of deep traps. *IEEE Trans. Dielectr. Electr. Insul.* **2016**, *23*, 564–572. [[CrossRef](#)]

**Disclaimer/Publisher’s Note:** The statements, opinions and data contained in all publications are solely those of the individual author(s) and contributor(s) and not of MDPI and/or the editor(s). MDPI and/or the editor(s) disclaim responsibility for any injury to people or property resulting from any ideas, methods, instructions or products referred to in the content.